

**REPORT ON TOYOTA/PRIUS MOTOR  
TORQUE CAPABILITY, TORQUE  
PROPERTY, NO-LOAD BACK EMF, AND  
MECHANICAL LOSSES**

**J. S. Hsu, Ph.D.**

**C. W. Ayers**

**C. L. Coomer**

**R. H. Wiles**

**Oak Ridge National Laboratory**

**S. L. Campbell**

**K. T. Lowe**

**R. T. Michelhaugh**

**Oak Ridge Institute for Science and Education**

This report was prepared as an account of work sponsored by an agency of the United States Government. Neither the United States Government nor any agency thereof, nor any of their employees, makes any warranty, express or implied, or assumes any legal liability or responsibility for the accuracy, completeness, or usefulness of any information, apparatus, product, or process disclosed, or represents that its use would not infringe privately owned rights. Reference herein to any specific commercial product, process, or service by trade name, trademark, manufacturer, or otherwise, does not necessarily constitute or imply its endorsement, recommendation, or favoring by the United States Government or any agency thereof. The views and opinions of authors expressed herein do not necessarily state or reflect those of the United States Government or any agency thereof.

**Engineering Science & Technology Division**

**REPORT ON TOYOTA/PRIUS MOTOR TORQUE CAPABILITY,  
TORQUE PROPERTY, NO-LOAD BACK EMF, AND  
MECHANICAL LOSSES**

J. S. Hsu, Ph.D.  
C. W. Ayers  
C. L. Coomer  
R. H. Wiles  
S. L. Campbell  
K. T. Lowe  
R. T. Michelhaugh

Publication Date: September 2004

Prepared by the  
OAK RIDGE NATIONAL LABORATORY  
Oak Ridge, Tennessee 37831  
managed by  
UT-BATTELLE, LLC  
for the  
U.S. DEPARTMENT OF ENERGY  
Under contract DE-AC05-00OR22725

In today's hybrid vehicle market, the Toyota Prius drive system is currently considered the leader in electrical, mechanical, and manufacturing innovations. It is significant that in today's marketplace, Toyota is able to manufacture and sell the vehicle for a profit.

This project's objective is to test the torque capability of the 2004 Prius motor and to analyze the torque properties relating to the rotor structure. The tested values of no-load back electromotive force (emf) and mechanical losses are also presented.

## PUBLISHED TORQUE CAPABILITY OF THE TOYOTA/PRIUS MOTOR

In today's hybrid vehicle market, the Toyota/Prius motor has one of the highest-power-density traction motors.

Figure 1 shows the published comparison of the output power and torque versus speed between the 2003 (THS) model and 2004 (THSII) model of the Prius motors. Both the output power and the torque of the motor are significantly increased in the new model.

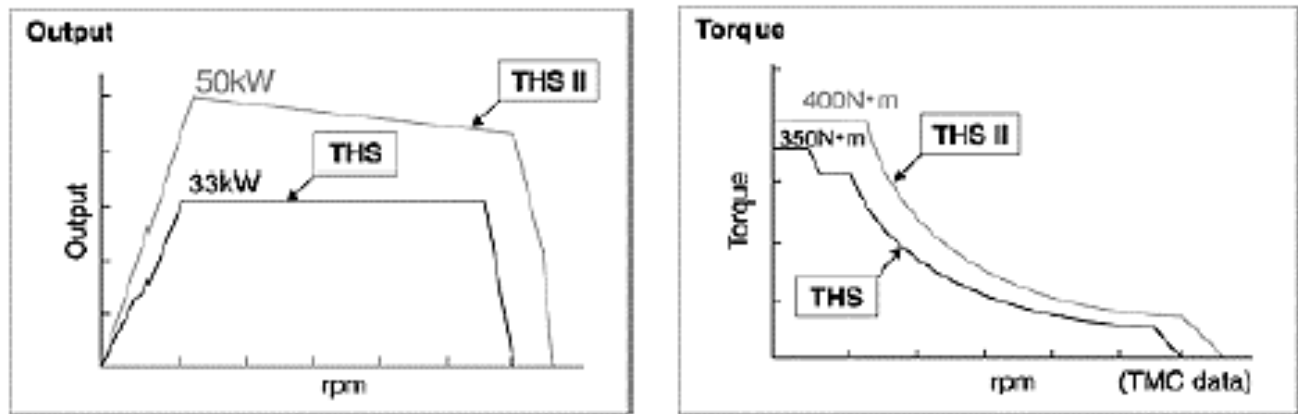


**Fig. 1. Comparison of output power and torque versus speed between the 2003 (THS) and 2004 (THSII) Prius motors.**

**Source:** *Development of Hybrid Electric Drive System Using a Boost Converter*, Masaki Okamura, Eiji Sato, and Shoichi Sasaki, Toyota Motor Corporation.

The power at base speed as tabulated in Table 1 is 50 kW. This is significantly higher than the 33 kW of the older model. The torque of 400 Nm is also higher than the 350/305 Nm of the previous year's model.

**Table 1. Power and torque of the permanent magnet synchronous motor of Toyota/Prius hybrid THS and THS II systems**

	Model (2004)	Model (2003)
Power:	50 kW	33 kW
	at base speed	1040–5600 rpm
Torque:	400 Nm	350Nm 305 Nm
	up to base speed	0–400 rpm 400–1000rpm

In Toyota's publications, the authors have not found the distinctions between the continuous rating and the peak-power rating. Temperature-rise tests will be conducted to find out the continuous rating and the permissible time for the peak rating.

## TORQUE PROPERTY OF PERMANENT MAGNET (PM) RELUCTANCE MOTOR

Figure 2 is a phasor diagram of the phase variables of a PM reluctance machine. The symbol  $V$  is phase voltage;  $I$ , phase current;  $E$ , phase back-emf; suffix  $d$ , direct axis;  $q$ , quadrature axis; and  $\delta$ , load angle. The assumptions of sinusoidal time and space variables are used in the phasor diagram of Fig. 2. The 3-phase power,  $P$ , going into the motor is derived through the products of the voltage projections and the currents.

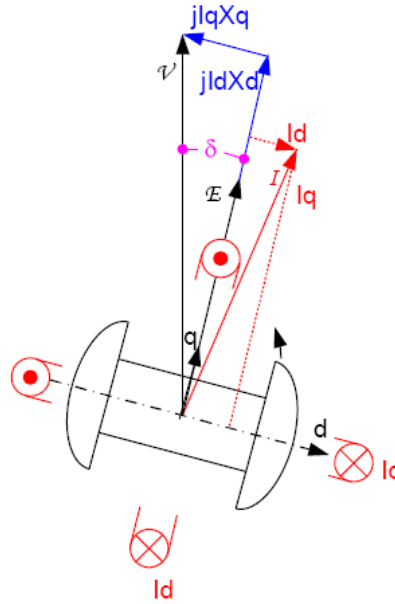


**Fig. 2. Phasor diagrams and symbol definitions of a PM reluctance motor.**

$$P = 3 (V \cos \delta I_q - V \sin \delta I_d). \quad (1)$$

The  $V \cos \delta$  and the  $V \sin \delta$  terms of Eq. (1) can be rewritten according to Fig. 2. This gives

$$P = 3 [(E + I_d X_d) I_q - I_q X_q I_d]. \quad (2)$$

Substituting  $I_d = (V \cos \delta - E)/X_d$ , and  $I_q = (V \sin \delta)/X_q$  into Eq. (2) gives

$$P = 3 [VE \sin \delta / X_d + 0.5 \sin 2\delta (1/X_q - 1/X_d)]. \quad (3)$$

The first term inside the brackets of Eq. (3) represents the synchronous power corresponding to the PMs that is proportional to  $\sin \delta$ . The second term is a typical reluctance power that varies according to  $\sin 2\delta$  and results from the difference of the reciprocals of the quadrature-axis and direct-axis reactances.

One of the design goals of the Toyota/Prius motor is to increase the difference between the quadrature-axis and the direct-axis reactances, yet retain a sufficiently high synchronous PM power.

The motor shaft output power is the product of the motor torque and the angular frequency of the shaft rotation. At zero speed, regardless of how high the torque is, the shaft output power is zero, because the angular frequency of the shaft is zero.

The torque of a PM reluctance motor such as the Prius motor is developed through the interaction between the armature current and the flux produced by the PMs and the reluctance paths. At zero speed, although the shaft output power is zero, the power of the PMs and the difference between the quadrature- and direct-axis inductances are already established. These power derivations can be applied to the PM and reluctance torques that are proportional to the  $\sin\delta$  and the  $\sin 2\delta$ , respectively. For the same reason, the motor torque capability obtained at zero speed serves as a good indicator of the motor behavior throughout the motor's speed range.

The torque capability of the motor measured at zero speed is relatively simple to obtain. This is accomplished by separating the tested torque into its fundamental and second harmonic components. The fundamental component will indicate the PM torque component, and the second-order harmonic will represent the additional reluctance torque produced by the reluctance difference.

## TEST SETUP

Figure 3 shows the assembly of the Toyota/Prius hybrid THS II drive train system.

As shown in Fig. 3, the motor of the Toyota/Prius is not a stand-alone motor. The motor shaft is coupled to a set of gears and then to the wheel shafts without a direct motor-torque shaft coming out from the frame. The non-driving side motor shaft is not strong enough for loading but can be coupled for the rotor position indication. Because the two wheel axle shafts are the outputs of a differential gear set driven by the motor, the locked torque of the motor can be measured through a torque gauge at one of the two wheel shafts when the other wheel shaft is locked. The torque ratio from the motor shaft to the wheel is determined by the revolution ratio between the wheel shaft and the motor shaft. For the Toyota/Prius hybrid THS II drive train system being tested, the torque at the wheel axle shaft multiplied by 0.486 gives the motor torque.

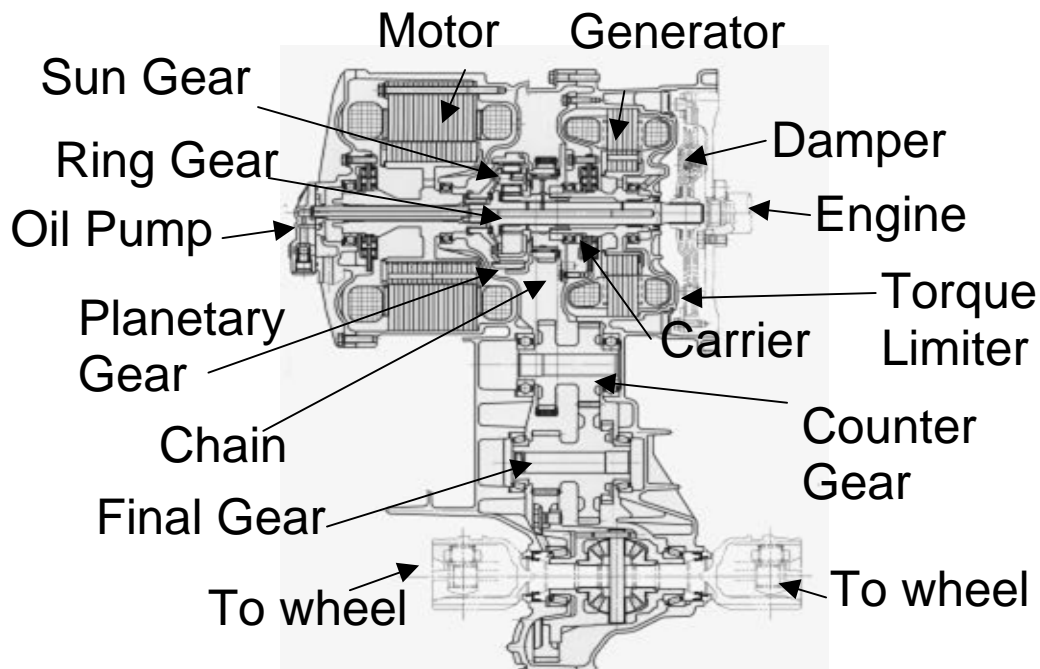


**Fig. 3. Motor, generator, and engine of the 2004 Toyota/Prius hybrid THS II system.**

**Source:** *Development of Electric Motors for the TOYOTA Hybrid Vehicle "PRIUS,"* Kazuaki Shingo, Kaoru Kubo, Toshiaki Katsu, and Yuji Hata, Toyota Motor Corporation.

Figure 4 shows the test setup. Starting from the left side of the figure, one side of the torque gauge is coupled to a load adjustment arm. The angular position of the arm can be adjusted by a jack bolted to the end of the arm. The other side of the torque gauge is coupled to one of the two wheel axial shafts coming out from the motor and drive-train housing.

The load adjustment arm and the coarse angle indicators viewed from the end of the torque gauge are shown in Fig. 5. The coarse rotor angle indicators can only be used as a reference for the coarse adjustment of the rotor position, because the wheel axle shaft has a significant twist under a high torque. The directions of the jack's controlled movements are also indicated in the figure.

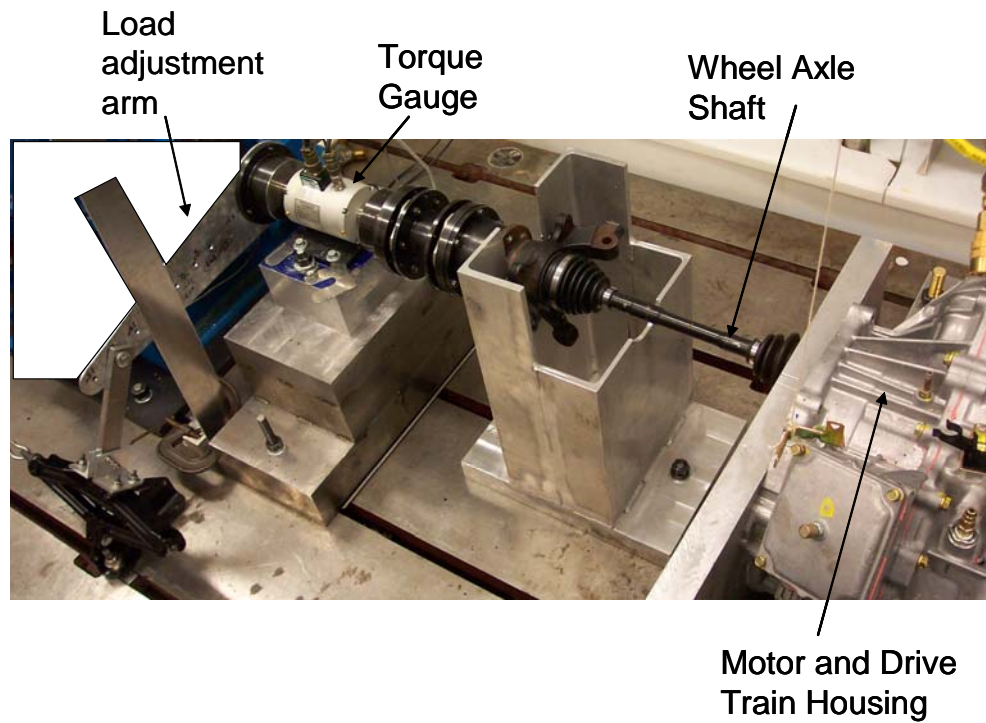


Fig. 4. Test setup.

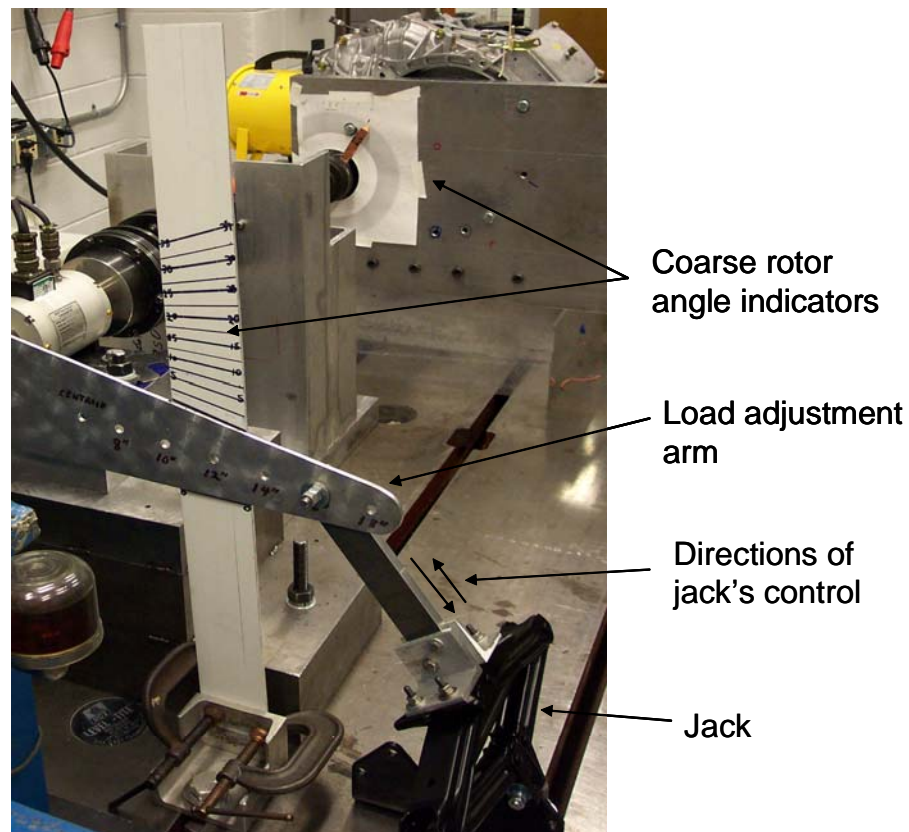
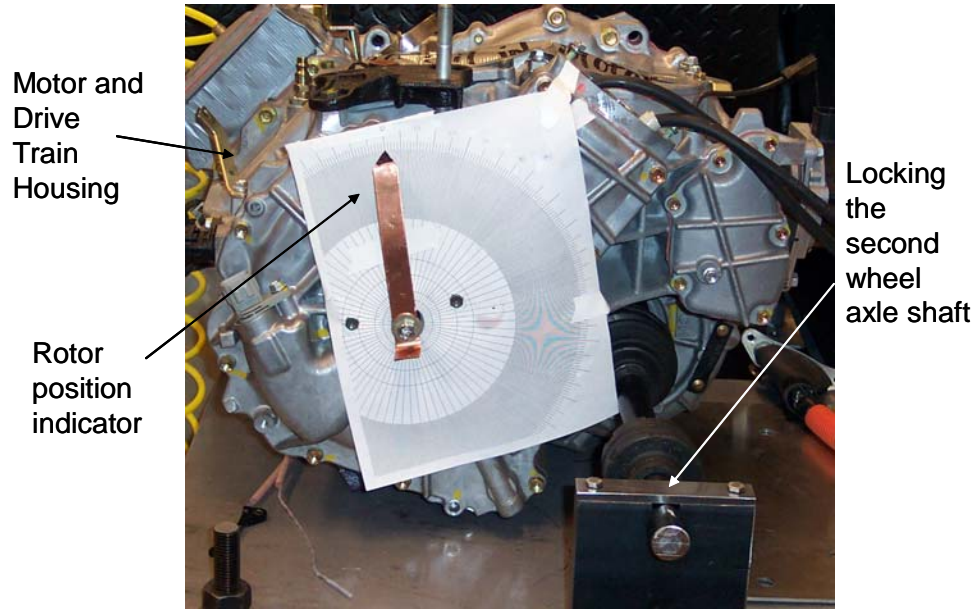


Fig. 5. Load torque adjustment mechanism during torque test.

Figure 6 illustrates the setup viewed from the end of the motor and drive train housing. The second wheel axle shaft is mechanically locked. A pointer is attached to the motor shaft's non-drive side. The rotor angular displacement can be accurately obtained from this setup. The zero position refers to the position without any load torque.



**Fig. 6. Pointer is attached to non-driving side shaft of motor.**

## **POWER SUPPLY FOR CONDUCTING MOTOR TORQUE CAPABILITY TEST AT ZERO SPEED**

Unlike in an induction motor that requires a rotating stator field to produce a rotor current, the power of the PMs and the reluctance difference between the direct and quadrature axes of the Prius motor are established without relying on the rotating stator field. Figure 7 shows a snapshot of the three-phase current phasors rotating at the synchronous speed for this motor torque capability test. Their projections to the vertical coordinate represent their instantaneous current values.

The instantaneous values at the instance shown in Fig. 7 are  $I_a$  for phase a,  $-0.5 \cdot I_a$  for phase b, and  $-0.5 \cdot I_a$  for phase c. These values will be used for the stator armature currents throughout the test.

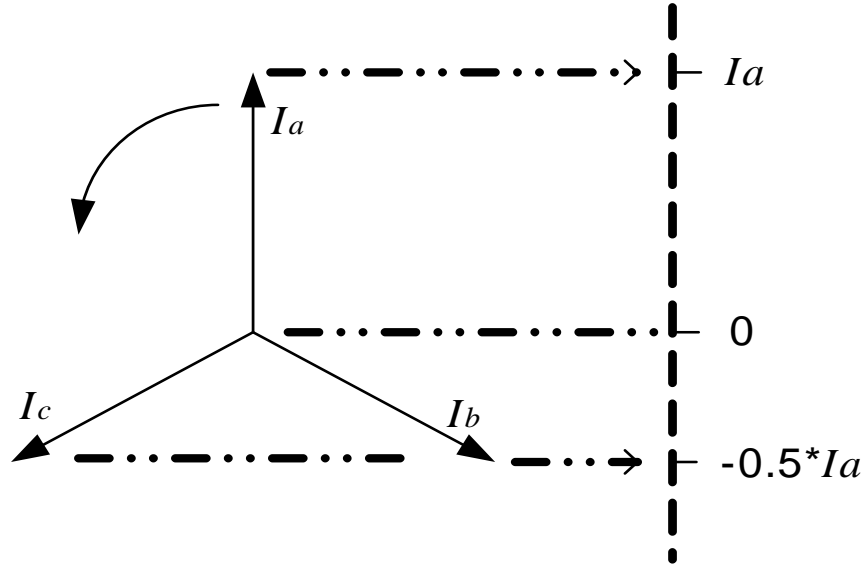


**Fig. 7. Three-phase current phasors and their instantaneous current values.**

A dc power supply can be used to supply the needed currents for the three phases, as shown in the circuit diagram of Fig. 8. The phase-a current would be divided into two halves that go through the phase b and c windings in an opposite direction from the phase-a current direction.

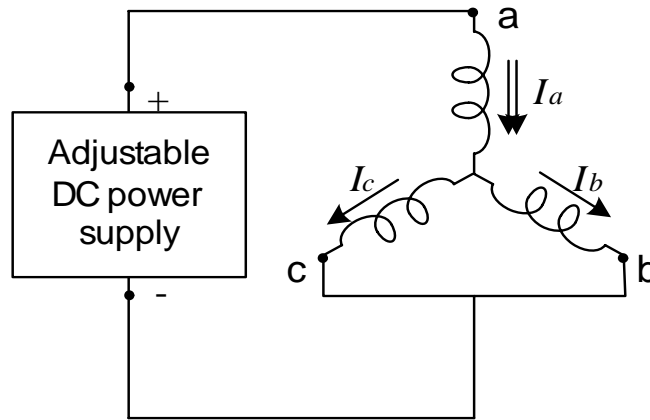


**Fig. 8. Circuit diagram for motor torque-capability test.**

### MEASURED TORQUE OF TOYOTA/PRIUS 2004 MOTOR

Figure 9 shows the motor torque versus the rotor mechanical angle away from the no-torque (or zero angle) position tested at 75, 150, 200, and 250 A, respectively. The motor is an 8-pole motor; therefore, the electrical angle is four times the mechanical angle. An amplitude of 250 A is required to produce the 400-Nm torque.

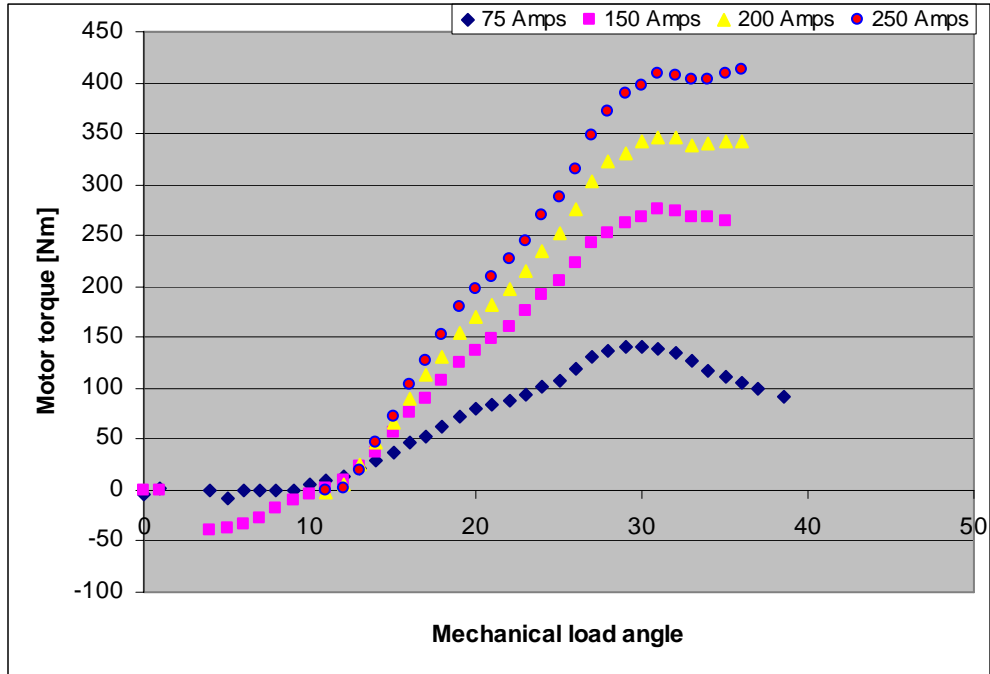


Fig. 9. Motor torque versus mechanical load angle of an 8-pole Prius motor at various currents.

#### MOTOR TORQUE-PROPERTY ANALYSES

The peak torque values versus current magnitudes are plotted in Fig. 10. A saturation of torque production gradually takes place as the current goes up. It is expected that when the current amplitude goes higher than 250 A, the torque saturation will become more significant.

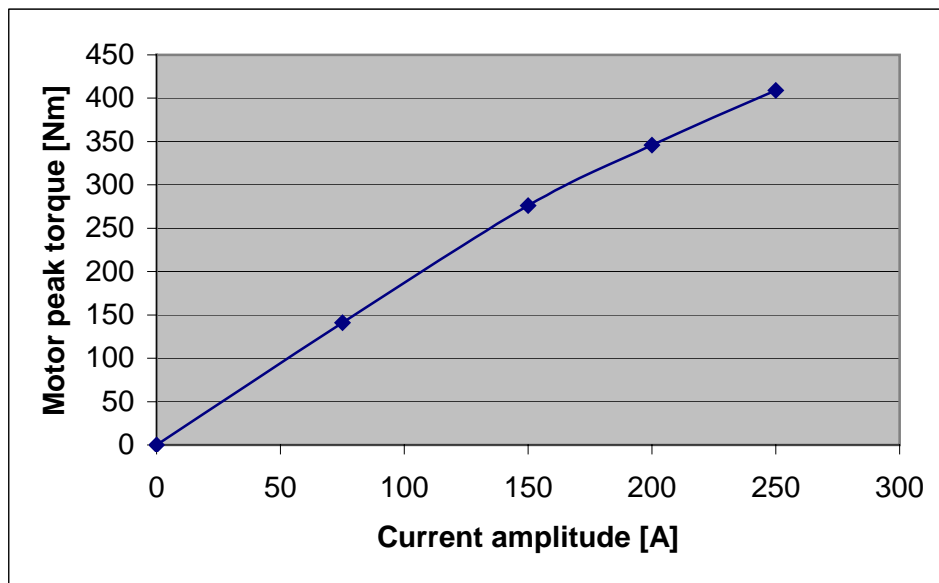
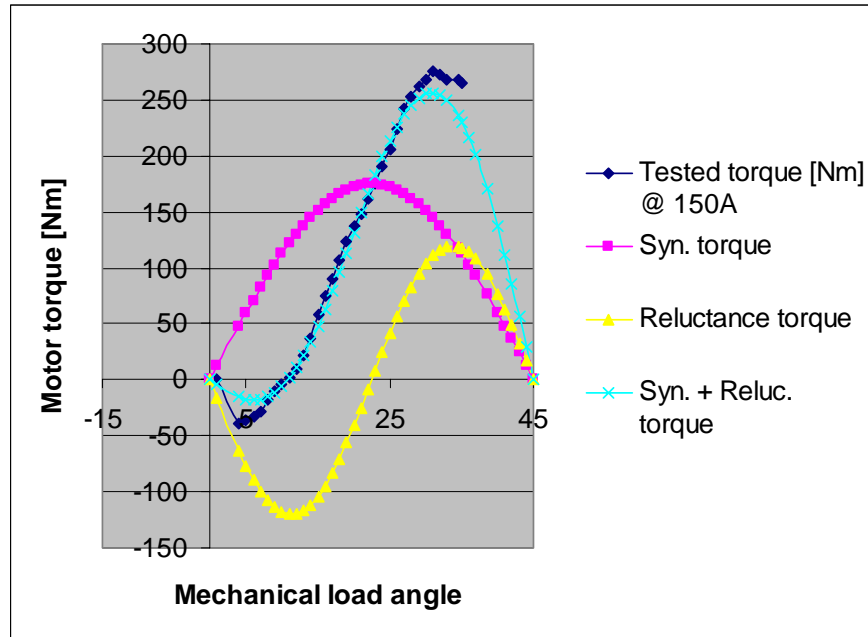


Fig. 10. Motor peak torque values versus the motor current amplitude.

As an example, Fig. 11 shows that at the phase current amplitude of 150 A, the tested motor torque can be broken down into a fundamental distribution and a second harmonic distribution. As explained, the fundamental distribution represents the synchronous PM torque, and the second harmonic distribution corresponds to the reluctance torque. In this case, the ratio of the amplitudes of the synchronous PM torque and the reluctance torque is 1.47 (176 Nm/120 Nm).



**Fig. 11. Tested torque of motor can be divided into synchronous and reluctance torques.**

The significant reluctance torque component is contributed by the rotor punching pattern shown in Fig. 12. It clearly shows a reluctance difference between the d and q axes. In this case, the q axis (i.e., located between the PM poles) allows the magnetic flux to go through easily. For this situation, when  $X_q$  is greater than  $X_d$ , the reluctance torque component versus load angle shown in Fig. 11 begins with the negative values.

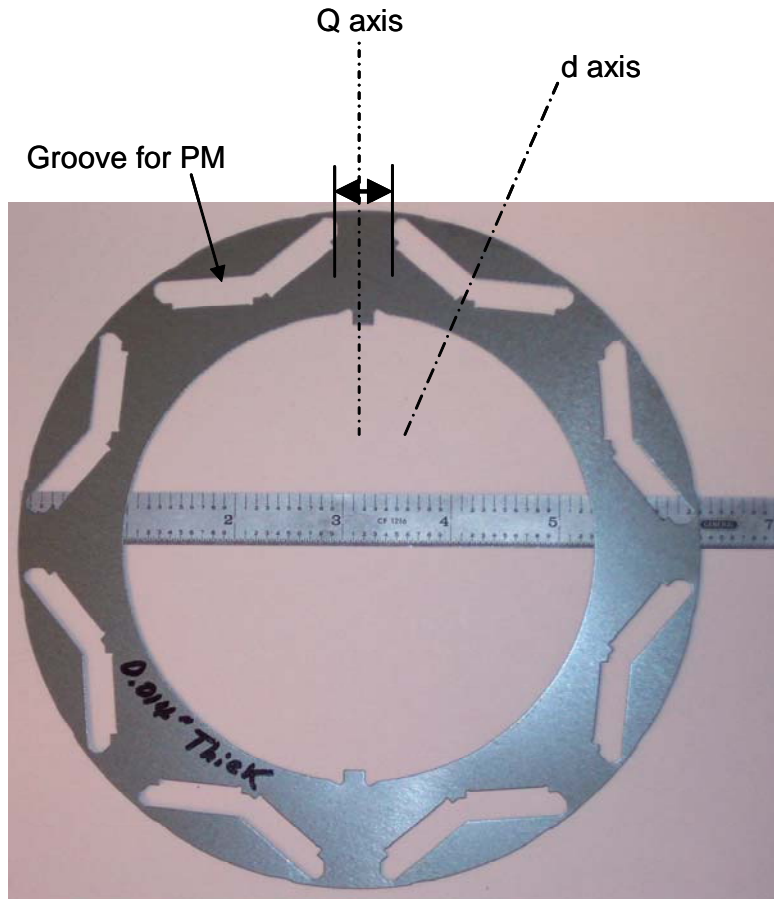


**Fig. 12. Prius 2004 rotor punchings.**

### **MEASURED BACK EMF**

The peak and rms values of the measured back emf versus motor speed are shown in Fig. 13. The peak voltage at 6000 rpm is 850 V. Because of the voltage harmonics, the ratio of the peak value and rms value is greater than 1.414 of the conventional sinusoidal waveforms.

At 3600 rpm, the back emf reaches 500 V. The Prius dc bus voltage can be boosted to 500 V, significantly lower than the value of 850 V obtained at 6000 rpm. This means that the Prius system has to rely on field weakening or current-angle advancement for a significant region at high speeds.

Because of the high back emf, the insulation requirement on the motor is high. Fortunately, the Prius motor uses direct oil cooling for its winding. The oil helps to increase the insulation strength.

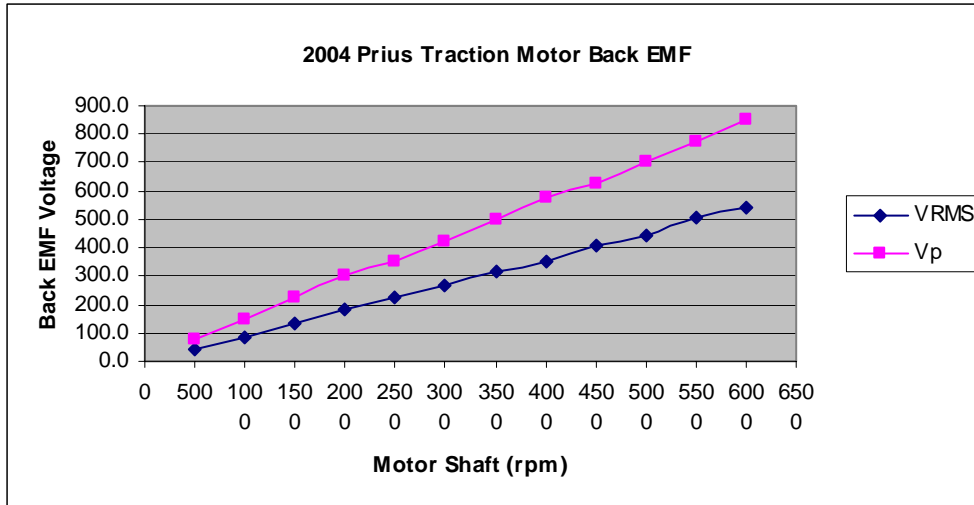


**Fig. 13. Measured back emfs versus speed.**

The measured back emf traces are illustrated in Fig. 14.

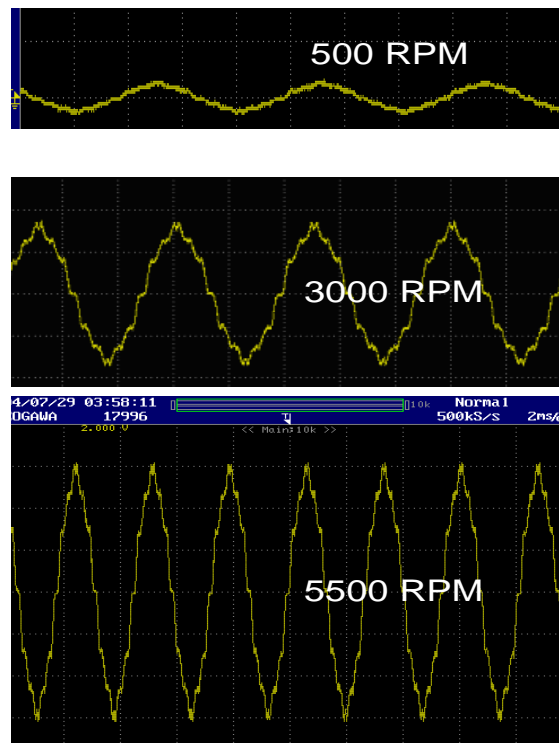


**Fig. 14. Back emfs of the Prius motor.**

The tested mechanical losses for the gears, rotor, and planetary, as well as the total losses, are plotted in Fig. 15. It is clear that the gear system produces significant losses. With a 30-kW load, the 2.4-kW mechanical losses calculate to a 7.4% (i.e.,  $100 \times 2.4 / (30 + 2.4) = 7.4\%$ ) efficiency drop at 6000 rpm. The mechanical losses are reduced at lower speeds.

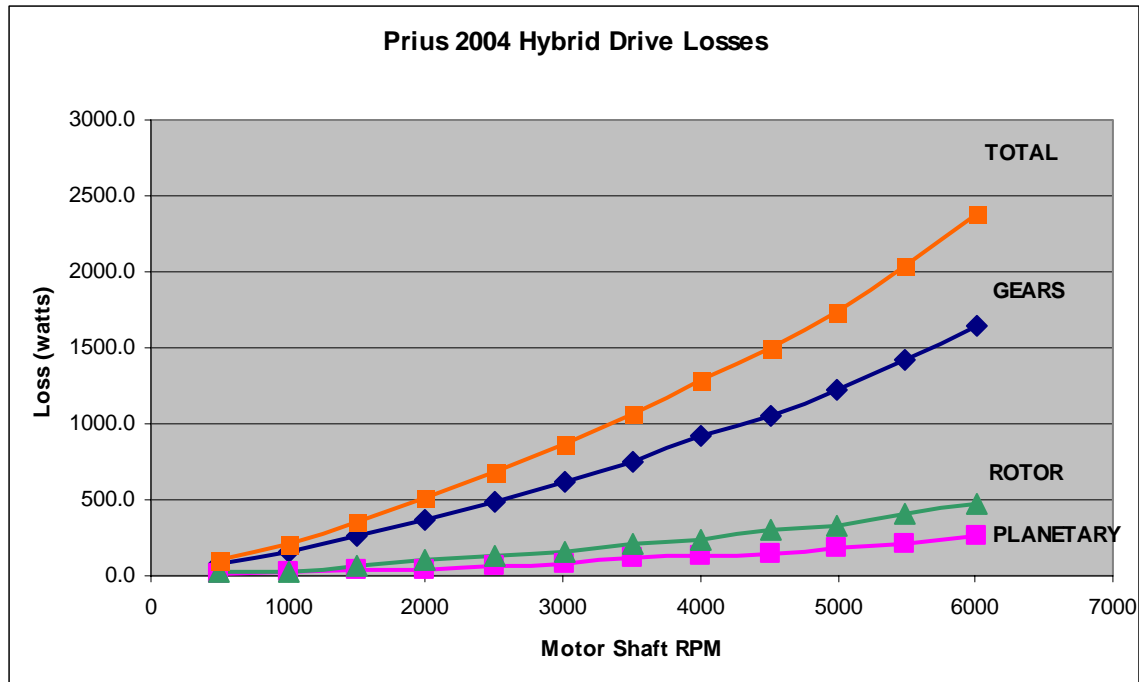


Fig. 15. The gear and motor mechanical losses.

## CONCLUSIONS

1. The motor torque capability test and the torque property analysis of the Toyota/Prius 2004 motor were conducted at the Oak Ridge National Laboratory. This report can be used as a reference for the torque-capability and torque-property assessments of similar types of motors (i.e., PM, reluctance, PM/reluctance, etc.).
2. The motor torque capability is a direct indicator of the motor power density.
3. The torque of a PM reluctance motor such as the Prius motor is developed through the interaction between the armature current and the flux produced by the PMs and the reluctance paths. At zero speed, although the shaft output power is zero, the PMs and the difference between the quadrature- and direct-axis inductances are already established. The motor torque capability obtained at zero speed serves as a good indicator of the motor's behavior throughout the motor's speed range.
4. The torque of the 2004 Prius motor can be separated into PM and reluctance torques that are proportional to the  $\sin\delta$  and the  $\sin 2\delta$ , respectively.
5. The torque versus motor load angle is measured by a torque gauge coupled to one of the two wheel axle shafts with the other wheel axle shaft locked. The load can be adjusted by shifting the angular position of the other end of the torque gauge.
6. The Prius motor meets the 400-Nm torque mentioned in Toyota's publication at zero speed. The current amplitude required to reach the torque is 250 A. The reluctance torque component is very significant. For the amplitude of the 150 A case, the ratio of the amplitudes of the synchronous PM torque component and the reluctance torque component is 1.47 (176 Nm/120 Nm).
7. The design of the rotor punching plays an important role in the torque production.
8. The back emf of the motor is quite high. At 3600 rpm, the back emf reaches 500 V; at 6000 rpm, it reaches 850 V. This means that in order to run the motor, the Prius system has to advance the current angle for a significant region at high speed.

9. Because of the high back emf, the insulation requirement for the motor is high. Fortunately, the Prius motor uses direct oil-droplet cooling for its windings. The oil helps to increase the insulation strength.
10. The gear system is a source of mechanical losses. At 6000 rpm, with a 30-kW load, the total mechanical loss (excluding the electromagnetic losses) of the motor and its gears is 7.4%. The mechanical loss decreases at lower speed.

## **DISTRIBUTION**

### Internal

- |                 |                           |
|-----------------|---------------------------|
| 1. D. J. Adams  | 7. K. Lowe                |
| 2. C. W. Ayers  | 8. L. D. Marlino          |
| 3. S. Campbell  | 9. J. W. McKeever         |
| 4. C. L. Coomer | 10. T. Michelhaugh        |
| 5. E. C. Fox    | 11. R. H. Wiles           |
| 6. J. S. Hsu    | 12–13. Laboratory Records |

### External

14. S. A. Rogers, U.S. Department of Energy, EE-2G/Forrestal Building, 1000 Independence Avenue, S.W., Washington, D.C. 20585.
15. E. J. Wall, U.S. Department of Energy, EE-2G/Forrestal Building, 1000 Independence Avenue, S.W., Washington, D.C. 20585.